

Control Barrier Function Synthesis for Nonlinear Systems with Dual Relative Degree

Gilbert Bahati, Ryan K. Cosner, Max H. Cohen, Ryan M. Bena, and Aaron D. Ames

Abstract—Control barrier functions (CBFs) are a powerful tool for synthesizing safe control actions; however, constructing CBFs remains difficult for general nonlinear systems. In this work, we provide a constructive framework for synthesizing CBFs for systems with *dual relative degree*—where different inputs influence the outputs at two different orders of differentiation; this is common in systems with orientation-based actuation, such as unicycles and quadrotors. In particular, we propose *dual relative degree CBFs (DRD-CBFs)* and show that these DRD-CBFs can be constructively synthesized and used to guarantee system safety. Our method constructs DRD-CBFs by leveraging the dual relative degree property—combining a CBF for an integrator chain with a Lyapunov function certifying the tracking of safe inputs generated for this linear system. We apply these results to dual relative degree systems, both in simulation and experimentally on hardware using quadruped and quadrotor robotic platforms.

I. INTRODUCTION

Control invariance has become a powerful descriptor of safety requirements in modern control systems, where tools such as reachability [1], [2], model-predictive control (MPC) [3], [4], and control barrier functions (CBFs) [5] provide a framework for synthesizing safety-critical controllers. These approaches come with various trade-offs that may lead to benefits/drawbacks in different situations. One benefit of CBFs over other techniques is their efficient online computation; however, generating valid CBFs – those consistent with the system dynamics – from user-defined safety requirements (e.g., position constraints) is a challenging problem. Recently, various methods have emerged that enable the systematic synthesis of CBFs for relevant classes of systems, such as chains of integrators [6], strict feedback systems [7], and partially feedback linearizable systems [8]. While effective in certain cases, each of these approaches imposes certain structural requirements on the system dynamics, which may not hold for systems of interest. Methods such as exponential [9] and high order CBFs [10] require less structure of the dynamics, but place more restrictive requirements on the safety constraints [11].

Another important class of methods for CBF synthesis are those leveraging reduced-order models (ROMs) – simplified representations of the original system – in which safe commands generated by ROMs are tracked by more complex full-order models [11], [12]. These methods generally avoid the difficulties in CBF synthesis by focusing on dramatically simplified systems, e.g., by modeling a quadrupedal robot as

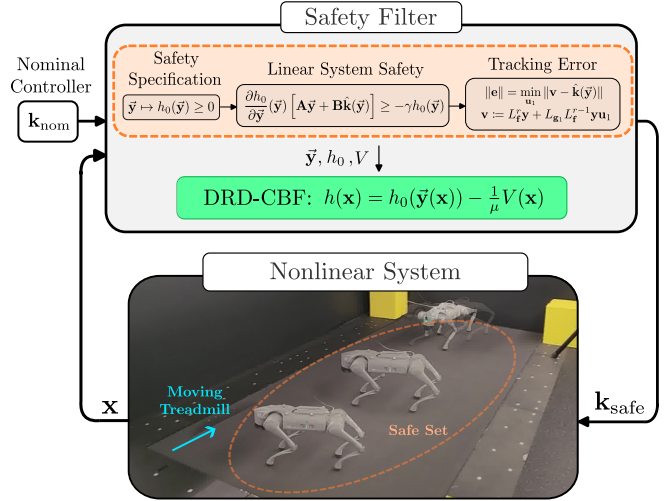


Fig. 1. A nominal control block diagram for enforcing safety constraints on a nonlinear system via DRD-CBFs. Hardware experiments can be viewed at <http://www.gbahati.com/cdc2025>.

a unicycle, and achieve system-level safety through the convergence of the full-order model to the ROM with sufficient tracking rates. Thus, safe-set synthesis can be performed on a simplified system and then extended to the full-order system without directly considering higher-order dynamics. While these synthesis methods are often conservative, they are capable of constructing control invariant subsets of user-defined safety requirements for rather complex systems.

User-defined safety requirements are often (sometimes implicitly) expressed through a choice of desired outputs, such as a system’s position in Euclidean space [8]. However, these outputs and their Lie derivatives may not fully capture all the system states (e.g., orientation), limiting the ability to control the entire system effectively. This often arises when the outputs do not possess a valid relative degree with respect to all the control inputs. In such a situation, it is often possible to dynamically extend the system to include higher derivatives of the inputs until a valid relative degree is achieved [13], and methods such as integral CBFs [14] may be leveraged for safety-critical control of dynamically extended systems [15]. However, the resulting integral-based controllers typically introduce delays to the nonlinear system. Dynamic extension is also closely related to techniques based on differential flatness [16], [17], which have demonstrated success in controlling highly dynamic systems such as quadrotors [18], [19]. Although there exists CBF synthesis methods tailored to specific differentially flat systems and safety constraints [20], [21], a general characterization of these ideas remains undeveloped.

This work is supported by BP and by TII under project #A6847.

The authors are with the Department of Mechanical and Civil Engineering, California Institute of Technology, Pasadena, CA {gbahati, rkcosner, maxcohen, ryanbena, ames}@caltech.edu.

Inspired by the above ideas, we propose a new method of synthesizing CBFs for a special, but relevant, class of systems – those with *dual relative degree*, where different components of the input influence the outputs at two different orders of differentiation—capturing systems such as unicycles and quadrotors. Compared to works like [8], this relaxes the requirement that the outputs must have a relative degree in the traditional sense. Rather than dynamically extending our system to achieve a valid relative degree and design a safe controller, we use a ROM-inspired approach [12] by leveraging a Lyapunov function to certify tracking of a class of linear systems by the nonlinear dynamics. The original safety constraint and this Lyapunov function enable the synthesis of a CBF for the full nonlinear system, yielding a *dual relative degree* CBF (DRD-CBF). From this perspective, our work can be seen as extending methods tailored for specific differentially flat systems and safety constraints [20], [21] to a wider class of systems and CBFs.

The main contributions of this work are three-fold. First, we provide a characterization of systems with *dual relative degree*. Second, we provide a constructive framework for synthesizing CBFs for these systems. Third, we illustrate the utility of our approach with in-depth case studies, including hardware demonstrations on quadrapeds and quadrotors.

II. TECHNICAL BACKGROUND

A. Control Barrier Functions

Consider¹ a nonlinear control-affine system of the form:

$$\dot{\mathbf{x}} = \mathbf{f}(\mathbf{x}) + \mathbf{g}(\mathbf{x})\mathbf{u}, \quad (1)$$

where $\mathbf{x} \in \mathbb{R}^n$ is the system state, $\mathbf{u} \in \mathbb{R}^m$ is the input, $\mathbf{f} : \mathbb{R}^n \rightarrow \mathbb{R}^n$ is the drift dynamics, and $\mathbf{g} : \mathbb{R}^n \rightarrow \mathbb{R}^{n \times m}$ is the actuation matrix. Using a state-feedback controller $\mathbf{k} : \mathbb{R}^n \rightarrow \mathbb{R}^m$, one obtains the closed-loop system:

$$\dot{\mathbf{x}} = \mathbf{f}_{\text{cl}}(\mathbf{x}) = \mathbf{f}(\mathbf{x}) + \mathbf{g}(\mathbf{x})\mathbf{k}(\mathbf{x}). \quad (2)$$

When the closed-loop dynamics are locally Lipschitz, they admit a unique continuously differentiable solution $t \mapsto \mathbf{x}(t)$ for any given initial state $\mathbf{x}_0 \in \mathbb{R}^n$, which, for ease of exposition, we assume exists for all $t \geq 0$. In this paper, we formalize the notion of safety using the concept of forward invariance. In particular, we consider safety requirements characterized by the forward invariance of some user-defined set $\mathcal{C} \subset \mathbb{R}^n$ given as the 0-superlevel set of some continuously differentiable function $h : \mathbb{R}^n \rightarrow \mathbb{R}$:

$$\mathcal{C} := \{\mathbf{x} \in \mathbb{R}^n \mid h(\mathbf{x}) \geq 0\}. \quad (3)$$

CBFs are one tool to synthesize control actions that enforce the forward invariance (i.e., safety) of this set \mathcal{C} .

Definition 1 (Control Barrier Function (CBF) [5]). A continuously differentiable function $h : \mathbb{R}^n \rightarrow \mathbb{R}$ defining a set

¹The Euclidean norm is denoted as $\|\cdot\|$. We denote that α is in the class of extended class- \mathcal{K} infinity functions as $\alpha \in \mathcal{K}_\infty^e$. For a full column/row rank matrix \mathbf{A} , we use \mathbf{A}^\dagger to denote the left/right Moore-Penrose pseudoinverse. With an abuse of terminology, we refer to a function as smooth if it is differentiable as many times as necessary.

$\mathcal{C} \subset \mathbb{R}^n$ as in (3) is a *control barrier function* (CBF) for (1) if there exists an $\alpha \in \mathcal{K}_\infty^e$ such that for all $\mathbf{x} \in \mathbb{R}^n$:

$$\sup_{\mathbf{u} \in \mathbb{R}^m} \left[\underbrace{\frac{\partial h}{\partial \mathbf{x}}(\mathbf{x})\mathbf{f}(\mathbf{x})}_{L_{\mathbf{f}}h(\mathbf{x})} + \underbrace{\frac{\partial h}{\partial \mathbf{x}}(\mathbf{x})\mathbf{g}(\mathbf{x})\mathbf{u}}_{L_{\mathbf{g}}h(\mathbf{x})} \right] > -\alpha(h(\mathbf{x})). \quad (4)$$

A CBF induces a point-wise set of safe inputs:

$$\mathcal{K}_{\text{CBF}}(\mathbf{x}) = \{\mathbf{u} \in \mathbb{R}^m \mid L_{\mathbf{f}}h(\mathbf{x}) + L_{\mathbf{g}}h(\mathbf{x})\mathbf{u} \geq -\alpha(h(\mathbf{x}))\},$$

such that any locally Lipschitz controller \mathbf{k} satisfying $\mathbf{k}(\mathbf{x}) \in \mathcal{K}_{\text{CBF}}(\mathbf{x})$ enforces forward invariance of \mathcal{C} [5]. Given a nominal controller $\mathbf{k}_{\text{nom}} : \mathbb{R}^n \rightarrow \mathbb{R}^m$, the following quadratic programming-based control law *filters* the nominal controller by minimally adjusting \mathbf{k}_{nom} to find the nearest safe action:

$$\begin{aligned} \mathbf{k}(\mathbf{x}) = \arg \min_{\mathbf{u} \in \mathbb{R}^m} \quad & \|\mathbf{u} - \mathbf{k}_{\text{nom}}(\mathbf{x})\|^2 && \text{(CBF-QP)} \\ \text{s.t.} \quad & L_{\mathbf{f}}h(\mathbf{x}) + L_{\mathbf{g}}h(\mathbf{x})\mathbf{u} \geq -\alpha(h(\mathbf{x})). \end{aligned}$$

While the above controller guarantees safety under ideal circumstances, it is often useful to robustify such controllers to unexpected disturbances. One tool for addressing this issue is an *input-to-state-safe CBF* (ISSf-CBF).

Definition 2 (ISSf-CBF [22]). A continuously differentiable function $h : \mathbb{R}^n \rightarrow \mathbb{R}$ is said to be an *input-to-state safe control barrier function* (ISSf-CBF) for (1) on \mathcal{C} as in (3) if there exists $\gamma > 0$ and $\varepsilon > 0$ such that for all $\mathbf{x} \in \mathbb{R}^n$:

$$\sup_{\mathbf{u} \in \mathbb{R}^m} [L_{\mathbf{f}}h(\mathbf{x}) + L_{\mathbf{g}}h(\mathbf{x})\mathbf{u}] > -\gamma h(\mathbf{x}) + \frac{\|L_{\mathbf{g}}h(\mathbf{x})\|^2}{\varepsilon}. \quad (5)$$

ISSf-CBFs include a robustness margin $\frac{1}{\varepsilon}\|L_{\mathbf{g}}h(\mathbf{x})\|^2$ to mitigate the impact of disturbances while providing practical safety guarantees [22]. Note that if h satisfies (4), then it also satisfies (5) as robustness is only added when there is control actuation available (i.e., when $\|L_{\mathbf{g}}h(\mathbf{x})\| \neq 0$). Thus, (5) increases the robustness of safety to disturbances while ensuring that $\mathcal{K}_{\text{CBF}}(\mathbf{x})$ remains nonempty.

B. Outputs and Coordinate Transformations

While CBFs provide a powerful approach for synthesizing safety-critical controllers, their success relies on knowledge of a function h satisfying Def. 1. In general, constructing CBFs for nonlinear systems can be mapped to a backwards reachability problem [23]; however, when the dynamics satisfy certain structural properties, the synthesis of CBFs can be made systematic [7], [8]. This structure may be revealed by selecting a set of outputs with a relative degree.

Definition 3 (Relative Degree r [13]). A smooth function $\mathbf{y} : \mathbb{R}^n \rightarrow \mathbb{R}^p$ has *relative degree* $r \in \mathbb{N}$ for (1) if:

$$L_{\mathbf{g}}L_{\mathbf{f}}^i\mathbf{y}(\mathbf{x}) \equiv \mathbf{0}, \quad \forall i \in \{0, \dots, r-2\}, \quad (6)$$

$$\text{rank}(L_{\mathbf{g}}L_{\mathbf{f}}^{r-1}\mathbf{y}(\mathbf{x})) = p, \quad \forall \mathbf{x} \in \mathbb{R}^n. \quad (7)$$

Given an output with relative degree r , define:

$$\vec{\mathbf{y}}(\mathbf{x}) := [\mathbf{y}(\mathbf{x})^\top \ L_{\mathbf{f}}\mathbf{y}(\mathbf{x})^\top \ \dots \ L_{\mathbf{f}}^{r-1}\mathbf{y}(\mathbf{x})^\top]^\top \in \mathbb{R}^{pr}, \quad (8)$$

as a new set of partial coordinates with dynamics:

$$\frac{d}{dt}\bar{\mathbf{y}}(\mathbf{x}) = \underbrace{\begin{bmatrix} \mathbf{0} & \mathbf{I}_{p(r-1)} \\ \mathbf{0} & \mathbf{0} \end{bmatrix}}_{\mathbf{A}} \bar{\mathbf{y}}(\mathbf{x}) + \underbrace{\begin{bmatrix} \mathbf{0} \\ \mathbf{I}_p \end{bmatrix}}_{\mathbf{B}} \mathbf{v} \quad (9)$$

$$\mathbf{v} := L_{\mathbf{f}}^r \mathbf{y}(\mathbf{x}) + L_{\mathbf{g}} L_{\mathbf{f}}^{r-1} \mathbf{y}(\mathbf{x}) \mathbf{u}, \quad (10)$$

where (10) is viewed as an input to (9). The output dynamics in (9) are a chain of integrators and techniques such as [6], [7] may be employed to construct CBFs. Importantly, when \mathbf{y} has relative degree r , any controller $\mathbf{v} = \hat{\mathbf{k}}(\bar{\mathbf{y}})$ designed for (9) may be transferred back to (1) via:

$$\mathbf{u} = L_{\mathbf{g}} L_{\mathbf{f}}^{r-1} \mathbf{y}(\mathbf{x})^\dagger \left[\hat{\mathbf{k}}(\bar{\mathbf{y}}(\mathbf{x})) - L_{\mathbf{f}}^r \mathbf{y}(\mathbf{x}) \right], \quad (11)$$

where the right pseudo-inverse $L_{\mathbf{g}} L_{\mathbf{f}}^{r-1} \mathbf{y}(\mathbf{x})^\dagger$ exists given (7). When the output coordinates $\bar{\mathbf{y}}$ are physically relevant to the original safety specification for (1), this provides a systematic approach to synthesizing CBFs and safety-critical controllers for complex nonlinear systems. In general, however, the outputs relevant to the safety specification for (1) may not have a valid relative degree, precluding the ability to directly transfer inputs from the output integrator system (9) back to the nonlinear system (1) via the controller transformation (11). In what follows, we provide a framework for relating inputs of the output integrator system (9) to those of the nonlinear system (1) under weaker conditions than Def. 3, and demonstrate how this leads to the synthesis of CBFs for practically relevant systems.

III. MAIN THEORETICAL CONTRIBUTION

A. Systems with Dual Relative Degree

In this section, we present a methodology to synthesize CBFs and safety-critical controllers for systems whose outputs may not have a valid relative degree, but satisfy other desirable properties that enable the construction of CBFs. We characterize these systems using the notion of *dual relative degree*, which captures the situation in which inputs influence the outputs at two different orders of differentiation. To facilitate our approach, we assume that (1) has multiple control inputs, i.e., $m \geq 2$, and thus may be written as:

$$\dot{\mathbf{x}} = \mathbf{f}(\mathbf{x}) + \underbrace{\mathbf{g}_1(\mathbf{x}) \mathbf{u}_1 + \mathbf{g}_2(\mathbf{x}) \mathbf{u}_2}_{\mathbf{g}(\mathbf{x}) \mathbf{u}}, \quad (12)$$

where $\mathbf{u}_1 \in \mathbb{R}^{m_1}$, $\mathbf{u}_2 \in \mathbb{R}^{m_2}$ such that $m = m_1 + m_2$ with $\mathbf{u} = (\mathbf{u}_1, \mathbf{u}_2)$, while $\mathbf{g}_1 : \mathbb{R}^n \rightarrow \mathbb{R}^{n \times m_1}$ and $\mathbf{g}_2 : \mathbb{R}^n \rightarrow \mathbb{R}^{n \times m_2}$ decompose \mathbf{g} as $\mathbf{g}(\mathbf{x}) = [\mathbf{g}_1(\mathbf{x}) \quad \mathbf{g}_2(\mathbf{x})]$. Given these dynamics and an output $\mathbf{y} : \mathbb{R}^n \rightarrow \mathbb{R}^p$ for (12), the inputs affect these outputs via:

$$\underbrace{L_{\mathbf{g}} L_{\mathbf{f}}^i \mathbf{y}(\mathbf{x})}_{p \times m} = \left[\underbrace{L_{\mathbf{g}_1} L_{\mathbf{f}}^i \mathbf{y}(\mathbf{x})}_{p \times m_1} \quad \underbrace{L_{\mathbf{g}_2} L_{\mathbf{f}}^i \mathbf{y}(\mathbf{x})}_{p \times m_2} \right]. \quad (13)$$

Rather than requiring \mathbf{y} to have a relative degree, we will require it to have a dual relative degree, defined as follows:

Definition 4. (Dual Relative Degree) A multi-input system (12) with smooth output $\mathbf{y} : \mathbb{R}^n \rightarrow \mathbb{R}^p$ is said to have *dual relative degree* $(r, q) \in \mathbb{N} \times \mathbb{N}$ if (6) holds and for all $\mathbf{x} \in \mathbb{R}^n$:

$$L_{\mathbf{g}_2} L_{\mathbf{f}}^{r-1} \mathbf{y}(\mathbf{x}) = \mathbf{0}, \quad (14)$$

$$\text{rank}(L_{\mathbf{g}_1} L_{\mathbf{f}}^{r-1} \mathbf{y}(\mathbf{x})) = m_1, \quad (15)$$

$$\text{rank}(L_{\mathbf{g}_2} L_{\mathbf{f}}^{q-1} L_{\mathbf{g}_1} L_{\mathbf{f}}^{r-1} \mathbf{y}(\mathbf{x})) = m_2. \quad (16)$$

Dual relative degree systems represent those whose inputs influence the output at two different levels of differentiation, and capture systems such as unicycles and quadrotors. While we will not explicitly leverage (16), it is often implicit in our other assumptions (e.g., on the existence of a tracking control Lyapunov function in Def. 5) and is thus included to better characterize the systems to which our approach applies.

Similar to Def. 3, when (12) has a dual relative degree, we may define a set of output coordinates and corresponding output dynamics as in (8) and (9), respectively. However, when \mathbf{y} does not have a relative degree in the sense of Def. 3, there does not exist a one-to-one correspondence between inputs of (9) and (12). Despite this, if (12) has a dual relative degree, then given a desired controller $\hat{\mathbf{k}} : \mathbb{R}^{pr} \rightarrow \mathbb{R}^p$ for the linear output dynamics (9), we may find the input \mathbf{u}_1 which actuates the outputs in the manner closest to that of $\hat{\mathbf{k}}$ via least-squares minimization:

$$\begin{aligned} \mathbf{k}_1(\mathbf{x}) &:= \arg \min_{\mathbf{u}_1 \in \mathbb{R}^{m_1}} \|L_{\mathbf{f}}^r \mathbf{y}(\mathbf{x}) + L_{\mathbf{g}_1} L_{\mathbf{f}}^{r-1} \mathbf{y}(\mathbf{x}) \mathbf{u}_1 - \hat{\mathbf{k}}(\bar{\mathbf{y}}(\mathbf{x}))\|^2 \\ &= L_{\mathbf{g}_1} L_{\mathbf{f}}^{r-1} \mathbf{y}(\mathbf{x})^\dagger \left[\hat{\mathbf{k}}(\bar{\mathbf{y}}(\mathbf{x})) - L_{\mathbf{f}}^r \mathbf{y}(\mathbf{x}) \right], \end{aligned} \quad (17)$$

where $L_{\mathbf{g}_1} L_{\mathbf{f}}^{r-1} \mathbf{y}(\mathbf{x})^\dagger$ is the left pseudo-inverse, which exists under the rank assumption (15) from Def. 4. Taking $\mathbf{u}_1 = \mathbf{k}_1(\mathbf{x})$ produces the partial closed-loop system dynamics:

$$\dot{\mathbf{x}} = \mathbf{f}(\mathbf{x}) + \mathbf{g}_1(\mathbf{x}) \mathbf{k}_1(\mathbf{x}) + \mathbf{g}_2(\mathbf{x}) \mathbf{u}_2 \quad (18)$$

$$=: \mathbf{f}_1(\mathbf{x}) + \mathbf{g}_2(\mathbf{x}) \mathbf{u}_2. \quad (19)$$

While $\mathbf{k}_1(\mathbf{x})$ produces inputs closest to $\hat{\mathbf{k}}(\bar{\mathbf{y}}(\mathbf{x}))$, it may not be able to completely eliminate the error between the output actuation \mathbf{v} in (10) and the desired linear actuation $\hat{\mathbf{k}}(\bar{\mathbf{y}}(\mathbf{x}))$. We write this error explicitly as:

$$\begin{aligned} \mathbf{e}(\mathbf{x}) &:= L_{\mathbf{f}}^r \mathbf{y}(\mathbf{x}) + L_{\mathbf{g}_1} L_{\mathbf{f}}^{r-1} \mathbf{y}(\mathbf{x}) \mathbf{k}_1(\mathbf{x}) - \hat{\mathbf{k}}(\bar{\mathbf{y}}(\mathbf{x})), \quad (20) \\ &= (L_{\mathbf{g}_1} L_{\mathbf{f}}^{r-1} \mathbf{y}(\mathbf{x}) L_{\mathbf{g}_1} L_{\mathbf{f}}^{r-1} \mathbf{y}(\mathbf{x})^\dagger - \mathbf{I}) (\hat{\mathbf{k}}(\bar{\mathbf{y}}(\mathbf{x})) - L_{\mathbf{f}}^r \mathbf{y}(\mathbf{x})) \end{aligned}$$

which must be compensated for to ensure safety. This will be achieved using Lyapunov-based techniques.

Definition 5 (Tracking Control Lyapunov Function). A continuously differentiable function $V : \mathbb{R}^n \rightarrow \mathbb{R}_{\geq 0}$ is a *tracking control Lyapunov function* (CLF) for a control affine system (1) with respect to error function $\mathbf{e} : \mathbb{R}^n \rightarrow \mathbb{R}^{m_1}$ if there exists $\beta, \lambda > 0$ such that for all $\mathbf{x} \in \mathbb{R}^n$:

$$V(\mathbf{x}) \geq \beta \|\mathbf{e}(\mathbf{x})\|^2 \text{ and} \quad (21)$$

$$\inf_{\mathbf{u} \in \mathbb{R}^m} L_{\mathbf{f}} V(\mathbf{x}) + L_{\mathbf{g}} V(\mathbf{x}) \mathbf{u} \leq -\lambda V(\mathbf{x}). \quad (22)$$

We will use this tracking CLF to ensure convergence of our error $\mathbf{e}(\mathbf{x})$ to zero for the partial closed-loop system (19).

B. CBF Synthesis for Dual Relative Degree Systems

We now demonstrate how the paradigm in Sec. III-A may be used to synthesize safety-critical controllers. For this, we consider a dual relative degree system of the form (12) with an output $\mathbf{y} : \mathbb{R}^n \rightarrow \mathbb{R}^p$ and output dynamics (9,10). We then consider a desired safe set on the output coordinates $\bar{\mathbf{y}}$:

$$\mathcal{C}_{\mathbf{y}} := \{\mathbf{x} \in \mathbb{R}^n \mid h_0(\bar{\mathbf{y}}(\mathbf{x})) \geq 0\}, \quad (23)$$

and suppose that $h_0 : \mathbb{R}^{pr} \rightarrow \mathbb{R}$ is a CBF for (9) with \mathbf{v} viewed as a ‘‘virtual’’ input to the linear system. This assumption guarantees the existence of a smooth² controller $\hat{\mathbf{k}} : \mathbb{R}^{pr} \rightarrow \mathbb{R}^p$ enforcing the ISSf-CBF condition [24]:

$$\frac{\partial h_0}{\partial \bar{\mathbf{y}}}(\bar{\mathbf{y}}) \left[\mathbf{A}\bar{\mathbf{y}} + \mathbf{B}\hat{\mathbf{k}}(\bar{\mathbf{y}}) \right] > -\gamma h_0(\bar{\mathbf{y}}) + \frac{1}{\varepsilon} \left\| \frac{\partial h_0}{\partial \bar{\mathbf{y}}}(\bar{\mathbf{y}})\mathbf{B} \right\|^2, \quad (24)$$

for all $\bar{\mathbf{y}} \in \mathbb{R}^{pr}$ for some $\gamma, \varepsilon > 0$. While h_0 is a CBF for (9) with relative degree r , it is not necessarily a CBF for (12) with dual relative degree (r, q) , and it may be impossible to apply $\hat{\mathbf{k}}$ to (12) directly.

Inspired by the reduced-order model methods of [12], we synthesize a CBF for the system with dual relative degree (12) by augmenting h_0 with a scaled tracking CLF, $\frac{-1}{\mu}V(\mathbf{x})$ for some $\mu > 0$, to account for the error $\mathbf{e}(\mathbf{x})$ between \mathbf{k}_1 and $\hat{\mathbf{k}}$. We formally define this construction as:

Definition 6 (Dual Relative Degree CBF (DRD-CBF)). Consider system (12) with dual relative degree (r, q) . If $h_0 : \mathbb{R}^n \rightarrow \mathbb{R}$ is a CBF for the linear system (9) with degree r , $\hat{\mathbf{k}} : \mathbb{R}^n \rightarrow \mathbb{R}^p$ is a continuously differentiable function satisfying (24) for some $\gamma, \varepsilon > 0$, and $V : \mathbb{R}^n \rightarrow \mathbb{R}_{\geq 0}$ is a tracking control Lyapunov function for (18) with respect to error function (20) for some $\beta, \lambda > 0$, then the function:

$$h(\mathbf{x}) := h_0(\bar{\mathbf{y}}(\mathbf{x})) - \frac{1}{\mu}V(\mathbf{x}) \quad (25)$$

$$\text{with } \mu > 0 \text{ such that } \lambda \geq \gamma + \frac{\varepsilon\mu}{4\beta}, \quad (26)$$

is a *dual relative degree CBF* (DRD-CBF) for (12).

The condition in (26) dictates the relation between the convergence rate λ of the tracking CLF, the safety of h_0 (determined by $\hat{\mathbf{k}}$) via γ and the ISSf constant ε , and the scaling parameters μ and β . Intuitively, the condition (26) can be satisfied by increasing the error tracking speed of V by increasing λ , increasing the conservatism of $\hat{\mathbf{k}}$ by decreasing γ and ε , or by balancing the scaling of h_0 and V via μ or balancing the scaling V and \mathbf{e} via β .

Next, in Theorem 1, we prove that all DRD-CBFs are valid CBFs for system (12) by showing that the existence of control actions derived from $\hat{\mathbf{k}}$ and the tracking CLF certifies that (25) satisfies the CBF constraint (4). Thus, we show that DRD-CBFs are a special class of CBFs for dual relative

²As discussed in [8], [11], [24], the existence of CBF (or ISSf-CBF) satisfying (4) (or (5)) with a *strict* inequality guarantees the existence of a controller, as smooth as the dynamics and CBF, satisfying the corresponding barrier condition. Thus, if h_0 is a CBF for (9), we may, without loss of generality, construct a smooth feedback controller $\hat{\mathbf{k}}$ satisfying (24), with examples of such controllers available in [8], [11], [24].

degree systems that can be directly synthesized using a CBF h_0 for a linear integrator system (9) and a tracking CLF V .

Theorem 1. Consider a system of the form (12) with dual relative degree (r, q) . If $h : \mathbb{R}^n \rightarrow \mathbb{R}$ is a dual relative degree CBF for (12) as in (25), then it is also a CBF and any Lipschitz controller satisfying (4) for h renders $\mathcal{C} = \{\mathbf{x} \in \mathbb{R}^n \mid h(\mathbf{x}) \geq 0\} \subset \mathcal{C}_{\mathbf{y}}$ safe.

Proof. Computing the time-derivative of h_0 and bounding (omitting dependencies on \mathbf{x} for brevity) we obtain:

$$\dot{h}_0 = \frac{\partial h_0}{\partial \bar{\mathbf{y}}}(\bar{\mathbf{y}}) [\mathbf{A}\bar{\mathbf{y}} + \mathbf{B}\mathbf{v}] \quad (27)$$

$$= \frac{\partial h_0}{\partial \bar{\mathbf{y}}}(\bar{\mathbf{y}}) [\mathbf{A}\bar{\mathbf{y}} + \mathbf{B}\hat{\mathbf{k}}(\bar{\mathbf{y}})] + \frac{\partial h_0}{\partial \bar{\mathbf{y}}}(\bar{\mathbf{y}})\mathbf{B} [\mathbf{v} - \hat{\mathbf{k}}(\bar{\mathbf{y}})] > -\gamma h_0(\bar{\mathbf{y}}) + \frac{1}{\varepsilon} \left\| \frac{\partial h_0}{\partial \bar{\mathbf{y}}}(\bar{\mathbf{y}})\mathbf{B} \right\|^2 \quad (28)$$

$$- \left\| \frac{\partial h_0}{\partial \bar{\mathbf{y}}}(\bar{\mathbf{y}})\mathbf{B} \right\| \|\mathbf{v} - \hat{\mathbf{k}}(\bar{\mathbf{y}})\| \geq -\gamma h_0(\bar{\mathbf{y}}) - \frac{\varepsilon}{4} \|\mathbf{v} - \hat{\mathbf{k}}(\bar{\mathbf{y}})\|^2 \quad (29)$$

$$= -\gamma h_0(\bar{\mathbf{y}}) - \frac{\varepsilon}{4} \left\| L_{\mathbf{f}}^r \mathbf{y} + L_{\mathbf{g}_1} L_{\mathbf{f}}^{r-1} \mathbf{k}_1 - \hat{\mathbf{k}}(\bar{\mathbf{y}}) \right\|^2 \quad (30)$$

$$\geq -\gamma h_0(\bar{\mathbf{y}}) - \frac{\varepsilon}{4\beta} V = -\gamma h - \left(\frac{\gamma}{\mu} + \frac{\varepsilon}{4\beta} \right) V. \quad (31)$$

In the above expression, (27) follows directly from the linear output dynamics (9). Next, (28) is obtained by adding zero, assuming $\hat{\mathbf{k}}$ enforces the ISSf-CBF inequality (24) for (9), and applying the Cauchy-Schwartz inequality³. We then complete the square to achieve (29), and then use the definition of \mathbf{v} in (10) to rewrite (29) as (30). Next, we select \mathbf{k}_1 provided in (17) and use (21) to bound (30) using V . Finally, we use (25) to express h_0 in terms of h and V to yield (31).

Since V is a tracking CLF for (18), then, for each $\mathbf{x} \in \mathbb{R}^n$ there exists an input $\mathbf{u}_2 \in \mathbb{R}^{m_2}$ satisfying:

$$L_{\mathbf{f}_1} V(\mathbf{x}) + L_{\mathbf{g}_2} V(\mathbf{x})\mathbf{u}_2 \leq -\lambda V(\mathbf{x}). \quad (32)$$

Now, computing the time derivative of h with $\mathbf{u}_1 = \mathbf{k}_1(\mathbf{x})$ from (17) and bounding at each $\mathbf{x} \in \mathbb{R}^n$ using the above expression, we obtain:

$$\dot{h} = \dot{h}_0 - \frac{1}{\mu} \dot{V} = \dot{h}_0 - \frac{1}{\mu} \frac{\partial V}{\partial \mathbf{x}} [\mathbf{f} + \mathbf{g}_1 \mathbf{k}_1 + \mathbf{g}_2 \mathbf{u}_2] \quad (33)$$

$$= \dot{h}_0 - \frac{1}{\mu} \frac{\partial V}{\partial \mathbf{x}} [\mathbf{f}_1 + \mathbf{g}_2 \mathbf{u}_2] \geq \dot{h}_0 + \frac{\lambda}{\mu} V \quad (34)$$

$$> -\gamma h + \frac{1}{\mu} \left(\lambda - \gamma - \frac{\varepsilon\mu}{4\beta} \right) V \geq -\gamma h, \quad (35)$$

where we used the partial closed-loop dynamics (18) to rewrite \dot{h} in (33). We then select \mathbf{u}_2 that satisfies (32) to obtain the bound in (34). We then substitute the bound obtained in (31) for \dot{h}_0 to obtain the first bound in (35). Finally, applying the inequality (26) for λ yields the second

³Given $|\mathbf{a}^\top \mathbf{b}| \leq \|\mathbf{a}\| \|\mathbf{b}\|$ for all $\mathbf{a}, \mathbf{b} \in \mathbb{R}^n$, $\|\cdot\| := \|\cdot\|_2$. Setting $\mathbf{b} = -\mathbf{c}$ gives $-\mathbf{a}^\top \mathbf{c} \leq \|\mathbf{a}\| \|\mathbf{c}\| \leq \|\mathbf{a}\| \|\mathbf{c}\| \implies \mathbf{a}^\top \mathbf{c} \geq -\|\mathbf{a}\| \|\mathbf{c}\|$.

bound in (35). Given that this choice of \mathbf{u} guarantees $\dot{h}(\mathbf{x}, \mathbf{u}) > -\gamma(h(\mathbf{x}))$ for all $\mathbf{x} \in \mathbb{R}^n$, h is a valid CBF⁴ for (12). Furthermore, since h is a CBF for (12), any Lipschitz continuous controller that satisfies (4) renders \mathcal{C} safe [5, Cor. 2], and since $V(\mathbf{x}) \geq 0$, the safe set \mathcal{C} is contained in the desired safe set \mathcal{C}_y , $\mathcal{C} \subset \mathcal{C}_y$, so trajectories that are safe with respect to \mathcal{C} also remain in the desired safe set \mathcal{C}_y . \square

Remark 1. Theorem 1 and its proof are inspired by results on CBFs and reduced-order models [11], [12] in which CBFs for simple models are combined with Lyapunov functions certifying tracking of such models to establish safety of the overall system. Our CBF construction may also be seen through this lens: CBFs designed for a chain of integrators (9) are transferred to a high-dimensional nonlinear system with dual relative degree using Lyapunov-based techniques. Importantly, as demonstrated in the following sections, the conditions of Theorem 1 are shown to hold for relevant systems, such as quadrotors, allowing for systematic synthesis of safety-critical controllers for highly dynamic systems based on CBFs designed for a chain of integrators.

The preceding result requires the existence of a global CLF. Due to various factors (e.g., topological obstructions to continuous stabilization [25, Ch. 4]), such a CLF may not exist for a given system of interest (e.g., that with states evolving on a differentiable manifold), and (22) may only hold on a set $\mathcal{D} \subset \mathbb{R}^n$. While global stabilization in such a situation may not be possible, enforcing safety is still possible, as demonstrated in the following result.

Corollary 1. (Global Safety) *Let the conditions of Theorem 1 hold, but suppose that (22) only holds on a set $\mathcal{D} \subset \mathbb{R}^n$. Define $\mathcal{E} := \mathbb{R}^n \setminus \mathcal{D}$. Provided that for all $\mathbf{x} \in \mathcal{E}$:*

$$\begin{aligned} & \left[L_{\mathbf{g}_1} h_0(\vec{\mathbf{y}}(\mathbf{x})) = \frac{1}{\mu} L_{\mathbf{g}_1} V(\mathbf{x}) \right] \\ \implies & \left[L_{\mathbf{f}} h_0(\vec{\mathbf{y}}(\mathbf{x})) - \frac{1}{\mu} L_{\mathbf{f}} V(\mathbf{x}) \geq -\gamma h(\mathbf{x}) \right], \end{aligned} \quad (36)$$

then h is a CBF for (12).

Proof. We divide the proof by considering two cases:

Case 1: If $\mathbf{x} \in \mathcal{D}$, then (22) holds and Theorem 1 implies that (4) holds for all $\mathbf{x} \in \mathcal{D}$.

Case 2: If $\mathbf{x} \in \mathcal{E}$, then (22) does not hold and we must have $L_{\mathbf{g}_2} V(\mathbf{x}) = \mathbf{0}$ (i.e., if $L_{\mathbf{g}_2} V(\mathbf{x}) \neq \mathbf{0}$ at this point, then there always exists an input \mathbf{u}_2 satisfying (22)). Taking the time derivative of h at $\mathbf{x} \in \mathcal{E}$ yields:

$$\begin{aligned} \dot{h} &= L_{\mathbf{f}} h_0 - \frac{1}{\mu} L_{\mathbf{f}} V + \left(L_{\mathbf{g}_1} h_0 - \frac{1}{\mu} L_{\mathbf{g}_1} V \right) \mathbf{u}_1 - \frac{1}{\mu} L_{\mathbf{g}_2} V \mathbf{u}_2 \\ &= \underbrace{L_{\mathbf{f}} h_0 - \frac{1}{\mu} L_{\mathbf{f}} V}_{L_{\mathbf{f}} h(\mathbf{x})} + \underbrace{\left(L_{\mathbf{g}_1} h_0 - \frac{1}{\mu} L_{\mathbf{g}_1} V \right)}_{L_{\mathbf{g}_1} h(\mathbf{x})} \mathbf{u}_1, \end{aligned} \quad (37)$$

⁴Implicit in the fact that h satisfies (4) with a strict inequality is that $\frac{\partial h}{\partial \mathbf{x}}(\mathbf{x}) \neq \mathbf{0}$ for all $\mathbf{x} \in \partial \mathcal{C}$, a regularity condition needed to apply standard CBF results regarding forward invariance [5].

for all $\mathbf{x} \in \mathcal{E}$, where $\mathbf{g}(\mathbf{x}) = [\mathbf{g}_1(\mathbf{x}) \quad \mathbf{g}_2(\mathbf{x})]$. Provided that (36) holds, we have $L_{\mathbf{g}} h(\mathbf{x}) = \mathbf{0}$ implies that $L_{\mathbf{f}} h(\mathbf{x}) \geq -\gamma h(\mathbf{x})$ for all $\mathbf{x} \in \mathcal{E}$, which implies that (4) holds for all $\mathbf{x} \in \mathcal{E}$ (cf. [26]). Combining Cases 1 and 2, we have that (4) holds for all $\mathbf{x} \in \mathbb{R}^n$, implying that h is a CBF for (12). \square

Given h in (25), Theorem 1 and the above Corollary allow for synthesizing an optimization-based controller as in (CBF-QP) for any given $\gamma \in \mathbb{R}_{>0}$ and nominal controller \mathbf{k}_{nom} . The following sections provide case studies of systems that satisfy the conditions of Theorem 1 and Corollary 1.

IV. CASE STUDY: UNICYCLE WITH DRIFT

We begin by considering the unicycle system with drift:

$$\frac{d}{dt} \begin{bmatrix} x \\ y \\ \theta \end{bmatrix} = \underbrace{\begin{bmatrix} d_x \\ d_y \\ 0 \end{bmatrix}}_{\mathbf{f}(\mathbf{x})} + \underbrace{\begin{bmatrix} \cos(\theta) \\ \sin(\theta) \\ 0 \end{bmatrix}}_{\mathbf{g}_1(\mathbf{x})} v + \underbrace{\begin{bmatrix} 0 \\ 0 \\ 1 \end{bmatrix}}_{\mathbf{g}_2(\mathbf{x})} \omega, \quad (38)$$

where the state $\mathbf{x} = (x, y, \theta) \in \mathcal{X} = \mathbb{R}^2 \times \mathbb{S}^1$ defines the planar position and heading angle. The control input $\mathbf{u} = (\mathbf{u}_1, \mathbf{u}_2) = (v, \omega) \in \mathbb{R}^2$ represents the linear and angular velocities. The values $d_x, d_y \in \mathbb{R}$ represent constant drift, motivated by the unicycle operating on a treadmill (e.g. Fig. 2). Our control objective is to constrain the position of the unicycle. Thus, we take our outputs as $\mathbf{y}(\mathbf{x}) = (x, y) \in \mathbb{R}^2$, which do not have a valid relative degree in the sense of Def. 3. However, the unicycle with this choice of outputs has dual relative degree $(r, q) = (1, 1)$ as one may verify that $L_{\mathbf{g}_1} \mathbf{y}(\mathbf{x}) = [\cos(\theta) \quad \sin(\theta)]^\top$ and $L_{\mathbf{g}_2} L_{\mathbf{g}_1} \mathbf{y}(\mathbf{x}) = [-\sin(\theta) \quad \cos(\theta)]^\top$, which both have rank 1.

A. Safety Specification

We consider a safety requirement that ensures the unicycle remains within an ellipse centered at $\mathbf{y}_c = [x_c, y_c]^\top \in \mathbb{R}^2$:

$$h_0(\vec{\mathbf{y}}(\mathbf{x})) = 1 - (\mathbf{y}(\mathbf{x}) - \mathbf{y}_c)^\top P (\mathbf{y}(\mathbf{x}) - \mathbf{y}_c), \quad (39)$$

where $P = \text{diag}(p_1, p_2) \in \mathbb{R}^{2 \times 2}$ is a diagonal matrix and $p_1, p_2 \in \mathbb{R}_{>0}$ are the weights corresponding to the lengths of the major and minor axes of the ellipse. The output coordinates $\vec{\mathbf{y}}(\mathbf{x}) = \mathbf{y}(\mathbf{x})$ yield a single-integrator system of the form (9). We design a differentiable controller $\hat{\mathbf{k}} := [\hat{\mathbf{k}}_x, \hat{\mathbf{k}}_y]^\top : \mathbb{R}^2 \rightarrow \mathbb{R}^2$ satisfying (24) for the single integrator using the methods in [24]. We then leverage the single integrator controller $\hat{\mathbf{k}}$ to generate a safe linear velocity $v = \mathbf{k}_1(\mathbf{x})$ as in (17) for the unicycle.

B. Safety-Critical Control

Let $\tilde{\mathbf{k}}(\mathbf{x}) := \hat{\mathbf{k}}(\vec{\mathbf{y}}) - L_{\mathbf{f}} \mathbf{y} = [\hat{\mathbf{k}}_y(\vec{\mathbf{y}}) - d_y, \hat{\mathbf{k}}_x(\vec{\mathbf{y}}) - d_x]^\top$. We consider the tracking CLF:

$$V(\mathbf{x}) = \frac{\|\tilde{\mathbf{k}}(\mathbf{x})\|^2}{2} \text{tr}(\mathbf{I}_{2 \times 2} - \mathbf{R}(\theta_{\text{des}}(\mathbf{x}))^\top \mathbf{R}(\theta)), \quad (40)$$

where for $\|\tilde{\mathbf{k}}(\mathbf{x})\| \neq 0$, the direction of the vector $\tilde{\mathbf{k}}(\mathbf{x})$ provides the desired safe heading angle (i.e., safe yaw) as $\theta_{\text{des}}(\mathbf{x}) = \text{atan2}(\hat{\mathbf{k}}_y(\vec{\mathbf{y}}(\mathbf{x})) - d_y, \hat{\mathbf{k}}_x(\vec{\mathbf{y}}(\mathbf{x})) - d_x)$, while if $\|\tilde{\mathbf{k}}(\mathbf{x})\| = 0$, then $V(\mathbf{x}) = 0$, making $\theta_{\text{des}}(\mathbf{x})$ a free

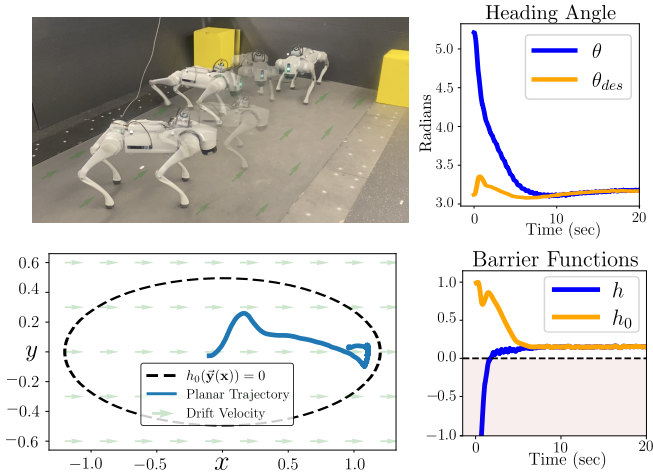


Fig. 2. **(top left)** The quadrupedal robot **(top right)** The yaw, θ , of the quadruped in blue and the desired yaw, θ_{des} , from the desired safe controller for the linear system $\hat{\mathbf{k}}(\bar{\mathbf{y}})$ in orange. **(bottom left)** (x, y) trajectories of the robot in blue with the drift velocity shown using green arrows and the boundary of \mathcal{C}_y (23) shown as a black dotted line. Notably, the trajectories stay in this set and satisfy our safety criterion as desired. **(bottom right)** Our DRD-CBF h in blue and the safety criterion h_0 in orange. Notably, h_0 remains above zero. The robot is initialized with an unsafe yaw θ , causing h to be initially negative (i.e., outside the safe set \mathcal{C} (3)). We demonstrate that the geometric tracking CLF (40) incorporated in h leads to the convergence of θ to a safe yaw θ_{des} yielding a positive h , enforcing attraction to \mathcal{C} .

parameter that may be assigned arbitrarily. The term $\mathbf{R} \in SO(2)$ is a 2D rotation matrix, so it follows that (40) yields:

$$V(\mathbf{x}) = \|\tilde{\mathbf{k}}(\mathbf{x})\|^2(1 - \cos(\theta - \theta_{des}(\mathbf{x}))), \quad (41)$$

which satisfies (21) as shown in the appendix.

We now consider the DRD-CBF as in (25), which we show is a CBF for (38). We first find that $L_{\mathbf{g}_2}V(\mathbf{x}) = 0 \implies \theta \in \{\theta_{des}(\mathbf{x}), \theta_{des}(\mathbf{x}) + \pi\}$. Let $\mu = 0.06$ and $\hat{\mathbf{k}}(\bar{\mathbf{y}}(\mathbf{x})) = -\rho P^{\frac{1}{2}}\mathbf{y}(\mathbf{x})$ with $\rho = 0.16$, then $L_{\mathbf{g}_1}h(\mathbf{x}) \neq 0$ when $\theta - \theta_{des}(\mathbf{x}) = \pi$ for all $\mathbf{x} \in \mathcal{C}_y$ defined in (23). Thus, Corollary 1 applies. Note that this does not imply global stability of θ on \mathbb{S}^1 with a continuous controller, but that there exists inputs for each $\mathbf{x} \in \mathcal{C}_y$ satisfying the CBF condition (4), ensuring safety but not necessarily stability of $\theta = \theta_{des}(\mathbf{x})$.

C. Unicycle: Simulation and Hardware

We demonstrate the effectiveness of our proposed CBF (25) in ensuring safety for system (38) in simulation and hardware. Using the safety specification (39), we synthesize a safe controller as in (CBF-QP) with the h defined in (25) for (38) with drift terms $d_x = 0.35$ m/s and $d_y = 0$. For the hardware demonstration, we apply this controller to a Unitree GO2 quadruped for which the unicycle may serve as a ROM⁵. On hardware, the drift terms are captured by placing the quadruped on a treadmill moving at a constant velocity of 0.35 m/s. The simulated and real-world trajectories can be seen ensuring safety in Fig. 2 with a nominal controller of zero linear and angular velocity.

⁵The velocity commands generated by our controller are then tracked by Unitree's onboard velocity tracking controller. In general, such an approach will lead to ISSf of the closed-loop system as analyzed in [11], [12].

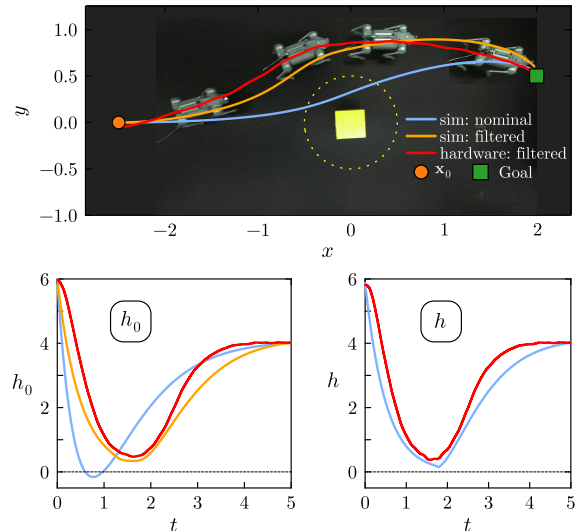


Fig. 3. Hardware (red) and simulated (orange and blue) unicycle trajectories. **(top)** A composite image showing the position of the quadruped throughout the experiment alongside position trajectories for the obstacle avoidance safe controller designed in Section IV-C on hardware (red) and in simulation, with the unfiltered \mathbf{k}_{nom} . **(bottom left)** The value of output safety requirement h_0 throughout the experiment. **(bottom right)** The value of the DRD-CBF h throughout the experiments.

To further illustrate our approach, we design a safe controller for (38) with no drift using $h_0 = h_{obs}$ as in (44) to avoid an obstacle with the nominal tracking controller $\mathbf{k}_{nom}(\mathbf{x}) = [K_p\|\mathbf{y}(\mathbf{x}) - \mathbf{y}_{des}\|, -K_q \sin(\theta - \theta_{des}(\mathbf{x}))]^T$ where $\mathbf{y}_{des} \in \mathbb{R}^2$ is a goal position and $K_p, K_q \in \mathbb{R}_{>0}$ are gains. This h_0 is used to construct a DRD-CBF h as in the previous subsection with $\hat{\mathbf{k}}$ satisfying (24), which satisfies the conditions of Theorem 1 and Corollary 1. Applying (CBF-QP) to this system using the corresponding h produces the results in Fig. 3, which shows this safe trajectory alongside the unfiltered \mathbf{k}_{nom} trajectory, which violates safety.

V. CASE STUDY: QUADROTOR

We now consider the quadrotor system, as discussed in [18], with the dynamics in the form (12) given by:

$$\frac{d}{dt} \begin{bmatrix} \mathbf{y} \\ \dot{\mathbf{y}} \\ \mathbf{q} \\ \boldsymbol{\omega} \end{bmatrix} = \underbrace{\begin{bmatrix} \dot{\mathbf{y}} \\ -g\mathbf{e}_z \\ \frac{1}{2}\mathbf{q} \otimes \boldsymbol{\omega}_q \\ \mathbf{0} \end{bmatrix}}_{\mathbf{f}(\mathbf{x})} + \underbrace{\begin{bmatrix} \mathbf{0} \\ \frac{1}{m}\mathbf{R}(\mathbf{q})\mathbf{e}_z \\ \mathbf{0} \\ -\mathbf{J}^{-1}\boldsymbol{\omega} \times \mathbf{J}\boldsymbol{\omega} \end{bmatrix}}_{\mathbf{g}_1(\mathbf{x})} \tau + \underbrace{\begin{bmatrix} \mathbf{0} \\ \mathbf{0} \\ \mathbf{0} \\ \mathbf{J}^{-1} \end{bmatrix}}_{\mathbf{g}_2(\mathbf{x})} \mathbf{M} \quad (42)$$

where $\mathbf{y} = (x, y, z) \in \mathbb{R}^3$ is the three dimensional position of the center of mass, $\mathbf{q} \in \mathbb{S}^3$ is the quaternion representing the orientation, $\boldsymbol{\omega}$ is the angular velocity in the body-fixed frame, and $\boldsymbol{\omega}_q = (0, \boldsymbol{\omega})$ is the pure quaternion representation of $\boldsymbol{\omega}$, $\mathbf{J} \in \mathbb{R}^{3 \times 3}$ is the inertia matrix with respect to the body-fixed frame, $m \in \mathbb{R}_{>0}$ is the total mass, $\tau \in \mathbb{R}$ is the total thrust, $\mathbf{M} \in \mathbb{R}^3$ is the total moment in the body-fixed frame, $g \in \mathbb{R}_{>0}$ is gravity, and \mathbf{e}_z is the inertial frame z -direction. Additionally, $\mathbf{R} \in SO(3)$ is the rotation matrix which can be derived from quaternion \mathbf{q} . The outputs $\mathbf{y} = (x, y, z)$ do not have a relative degree. Similar to the previous example, this system has dual relative degree $(r, q) = (2, 2)$ as both $L_{\mathbf{g}_1}L_f\mathbf{y}(\mathbf{x}) = \mathbf{R}(\mathbf{q})\mathbf{e}_z$ and $L_{\mathbf{g}_2}L_fL_{\mathbf{g}_1}L_f\mathbf{y}(\mathbf{x})$ have full rank.

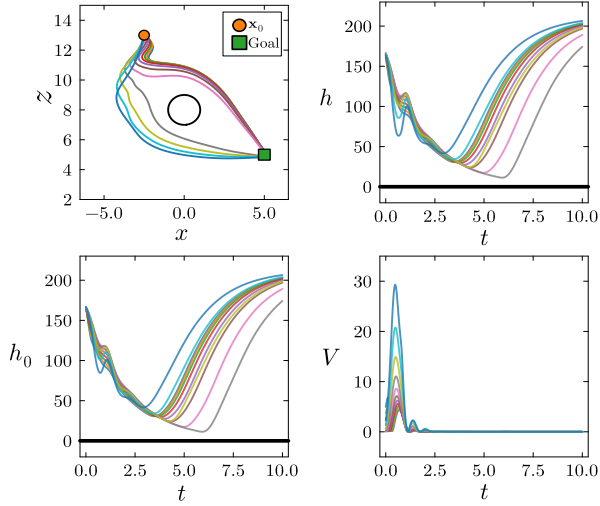


Fig. 4. 2D planar quadrotor simulation. **(top left)** Obstacle avoidance trajectories for various initial heading angles in the range $(0, \frac{3\pi}{4})$. **(bottom left)** The value of h_0 , derived from (44), which stays positive for all initial headings. **(top right)** The value of the DRD-CBF (25). **(bottom right)** The value of the attitude Lyapunov function V which is used to penalize h_0 .

Fixing the y position, and assuming unit inertial values, (42) reduces to the planar model of the quadrotor, where:

$$\mathbf{f}(\mathbf{x}) = [\dot{x}, \dot{z}, \omega, 0, -g, 0]^\top \quad (43a)$$

$$\mathbf{g}_1(\mathbf{x}) = [0, 0, 0, -\sin(\theta), \cos(\theta), 0]^\top \quad (43b)$$

$$\mathbf{g}_2(\mathbf{x}) = [0, 0, 0, 0, 0, 1]^\top \quad (43c)$$

with the state $\mathbf{x} = (x, z, \theta, \dot{x}, \dot{z}, \omega) \in \mathcal{X} = \mathbb{R}^2 \times \mathbb{S}^1 \times \mathbb{R}^3$ consisting of the quadrotor's horizontal position x , vertical position z , its orientation with respect to the horizontal plane θ , and their corresponding rates of change. The input to the system is $\mathbf{u} = (\mathbf{u}_1, \mathbf{u}_2) = (\tau, M) \in \mathbb{R}^2$ where τ denotes the total thrust and M denotes the total moment. Similar to the previous case study, our goal is to constrain the planar position of the quadrotor, captured by the outputs $\mathbf{y}(\mathbf{x}) = (x, z) \in \mathbb{R}^2$, which leads to a system with dual relative degree $(r, q) = (2, 2)$, where $L_{\mathbf{g}_1} L_{\mathbf{f}} \mathbf{y}(\mathbf{x}) = [-\sin(\theta), \cos(\theta)]^\top$ and $L_{\mathbf{g}_2} L_{\mathbf{f}} L_{\mathbf{g}_1} L_{\mathbf{f}} \mathbf{y}(\mathbf{x}) = [\cos(\theta), \sin(\theta)]^\top$.

A. Planar Quadrotor: Safety Specification

To avoid an obstacle at a position $\mathbf{y}_{\text{obs}} = [x_{\text{obs}}, y_{\text{obs}}] \in \mathbb{R}^2$ with radius $r_o \in \mathbb{R}_{>0}$, we consider the safety constraint:

$$h_{\text{obs}}(\mathbf{y}(\mathbf{x})) = \|\mathbf{y}(\mathbf{x}) - \mathbf{y}_{\text{obs}}\|^2 - r_o^2. \quad (44)$$

As this system has dual relative degree $(r, q) = (2, 2)$, the output coordinates are given by $\bar{\mathbf{y}}(\mathbf{x}) = (\mathbf{y}(\mathbf{x}), \dot{\mathbf{y}}(\mathbf{x})) = (x, z, \dot{x}, \dot{z})$ and yield double integrator dynamics of the form (9) for which techniques such as [6], [7], [10] may be employed to construct a CBF from h_{obs} . We construct a CBF $h_0 : \mathbb{R}^4 \rightarrow \mathbb{R}$ for a double-integrator using [7] and design a controller $\hat{\mathbf{k}} := [\hat{\mathbf{k}}_x, \hat{\mathbf{k}}_y]^\top : \mathbb{R}^4 \rightarrow \mathbb{R}^2$ satisfying (24) that generates a safe thrust $\tau = \mathbf{k}_1(\mathbf{x})$ as in (17) for the quadrotor.

B. Planar Quadrotor: Safety-Critical Control

As in the previous case study, when $\|\tilde{\mathbf{k}}(\mathbf{x})\| = \|\hat{\mathbf{k}}(\bar{\mathbf{y}}(\mathbf{x})) - L_{\hat{\mathbf{f}}}^2 \mathbf{y}(\mathbf{x})\| \neq 0$, we can define a desired safe heading angle as $\theta_{\text{des}}(\mathbf{x}) = \text{atan2}(\hat{\mathbf{k}}_y(\bar{\mathbf{y}}(\mathbf{x})) + g, \hat{\mathbf{k}}_x(\bar{\mathbf{y}}(\mathbf{x})))$ and consider a

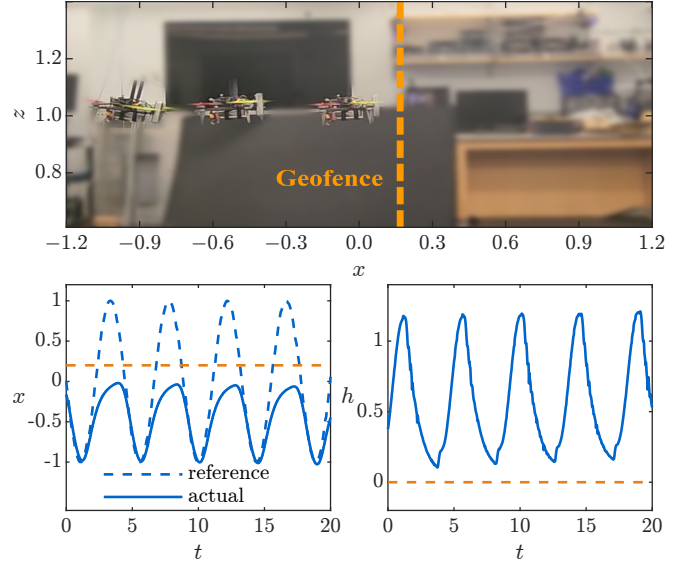


Fig. 5. 3D quadrotor demonstration. **(top)** A composite image showing the position of the quadrotor drone over the course of the geofencing experiment. **(bottom left)** The x -position reference, which passes beyond the geofence, and the actual x -position, which deviates from the reference to maintain safety. **(bottom right)** The value of the DRD-CBF (25), which stays positive throughout the flight, confirming that safety is maintained.

function as defined in (40), denoted by V_0 , whose derivative is of the form:

$$\dot{V}_0(\mathbf{x}) = \frac{\partial V_0}{\partial \bar{\mathbf{y}}}(\mathbf{x}) \dot{\bar{\mathbf{y}}} + \frac{\partial V_0}{\partial \theta}(\mathbf{x}) \omega. \quad (45)$$

However, since the quadrotor model (43) is a second-order system, we must design a moment M that drives ω to a desired state that ensures θ can be stabilized to $\theta_{\text{des}}(\mathbf{x})$. To achieve this, we construct a CLF using backstepping [27] as:

$$V(\mathbf{x}) = V_0(\mathbf{x}) + \frac{1}{2\mu_2} \|\omega - \mathbf{k}_\omega(\mathbf{x})\|^2, \quad (46)$$

with $\mu_2 > 0$, such that $\mathbf{k}_\omega : \mathbb{R}^n \rightarrow \mathbb{R}$ satisfies:

$$\frac{\partial V_0}{\partial \bar{\mathbf{y}}}(\mathbf{x}) \dot{\bar{\mathbf{y}}} + \frac{\partial V_0}{\partial \theta}(\mathbf{x}) \mathbf{k}_\omega(\mathbf{x}) \leq -\lambda V_0(\mathbf{x}). \quad (47)$$

One can verify that (46) satisfies (22) on a set \mathcal{X} for (43). We consider the DRD-CBF as in (25), and show that h is a CBF for (43). Using similar analysis to the previous case study, we observe that $L_{\mathbf{g}_2} V = 0 \implies \omega = \mathbf{k}_\omega(\mathbf{x})$ which, from (47), implies $\dot{V} = L_{\mathbf{f}_1} V \leq -\lambda V$, so the Lyapunov condition can be satisfied on all of \mathcal{X} . Again, note that we are not claiming that the Lyapunov condition (22) may be satisfied by a continuous controller, but that at each state, there exists inputs that render the system (43) safe, which is sufficient to ensure that h is a CBF as in Def. 1.

C. Planar Quadrotor: Simulation

We implement the above example in simulation with the safety-specification from (44) with a nominal tracking controller $\mathbf{k}_{\text{nom}}(\mathbf{x}) = [\mathbf{k}_1(\mathbf{x}), K_p(\theta_{\text{des}}(\mathbf{x}) - \theta) + K_q(\dot{\theta}_{\text{des}}(\mathbf{x}) - \omega)]^\top$ where $K_p, K_q \in \mathbb{R}_{>0}$ are gains. The resulting DRD-CBF is used to construct (CBF-QP) and Fig. 4 illustrates the trajectories of the planar quadrotor resulting from filtering \mathbf{k}_{nom} with h along with the satisfaction of safety and the tracking behavior encoded through the CLF.

D. 3D Quadrotor: Hardware

Finally, we deploy our method on a quadrotor drone. We use an OptiTrack motion capture system to provide the drone with real-time position measurements and a VectorNav VN-200 IMU for attitude state estimation. All state estimation and control computations are performed onboard at 750 Hz using a Jetson Orin NX. The drone model used is a simplified version of the dynamics (42) with thrust and desired angle rate inputs as in [28]. The desired angle rates are tracked by a Betaflight flight controller and ESC at 8 kHz.

To demonstrate the performance of our DRD-CBF (25), we command the quadrotor to track a sinusoidal reference $\mathbf{y}_d(t) = [-\sin(0.4\pi t), 0.0, 1.0]^\top$. We then define an x -coordinate geofence as the 0-superlevel set of $h_{\text{geo}}(\vec{\mathbf{y}}(\mathbf{x})) = x_{\text{geo}} - x$, where $x_{\text{geo}} \in \mathbb{R}$ is the x -position of the geofence [29]. For this particular experiment $x_{\text{geo}} = 0.2$ m. Using a high order CBF [9], [10], we extend h_{geo} to get h_0 , a CBF for the quadrotor double-integrator translational dynamics. By enforcing forward invariance of the safe-set defined by $h_0(\vec{\mathbf{y}}(\mathbf{x})) \geq 0$, we ensure the x -coordinate of the quadrotor never exceeds the value of x_{geo} , irrespective of the commanded reference. Select data are presented in Fig. 5 utilizing the DRD-CBF (25) with the tracking CLF (40) for 3D rotation matrices (see appendix).

From Fig. 5a and Fig. 5b, it is clear that the quadrotor drone effectively tracks the sinusoidal reference as long as it stays inside the safe set. However, once the commanded position crosses the geofence, the safety filter intercedes, preventing the drone from violating its safety specification.

VI. CONCLUSION

We presented a constructive framework for synthesizing CBFs and safety-critical controllers for nonlinear systems with dual relative degree, where outputs are used to specify safety requirements. We design a CBF for an integrator chain with a Lyapunov function to certify tracking of the safe inputs generated by this system, to synthesize a CBF for the full nonlinear system. We also provide a case study of systems of dual relative degree, for which we synthesize CBFs. We further demonstrated the efficacy of the proposed method on hardware platforms that exhibit these properties. Future work involves studying the impact of uncertainties in high-fidelity scenarios in navigation for this class of systems.

REFERENCES

- [1] S. Bansal, M. Chen, S. Herbert, and C. J. Tomlin, "Hamilton-Jacobi reachability: A brief overview and recent advances," in *Proc. Conf. Decis. Control*, pp. 2242–2253, 2017.
- [2] M. Chen, S. L. Herbert, H. Hu, Y. Pu, J. F. Fisac, S. Bansal, S. Han, and C. J. Tomlin, "Fastrack: A modular framework for real-time motion planning and guaranteed safe tracking," *IEEE Trans. Autom. Control*, vol. 66, no. 12, pp. 5861–5876, 2021.
- [3] F. Borrelli, A. Bemporad, and M. Morari, *Predictive control for linear and hybrid systems*. Cambridge University Press, 2017.
- [4] K. P. Wabersich and M. N. Wabersich, "Predictive control barrier functions: Enhanced safety mechanisms for learning-based control," *IEEE Trans. Autom. Control*, vol. 68, no. 5, pp. 2638–2651, 2023.
- [5] A. D. Ames, X. Xu, J. W. Grizzle, and P. Tabuada, "Control barrier function based quadratic programs for safety critical systems," *IEEE Trans. Autom. Control*, vol. 62, no. 8, pp. 3861–3876, 2017.

- [6] L. Doesser, P. Nilsson, A. D. Ames, and R. M. Murray, "Invariant sets for integrators and quadrotor obstacle avoidance," in *Proceedings of the American Control Conference*, pp. 3814–3821, 2020.
- [7] A. J. Taylor, P. Ong, T. G. Molnar, and A. D. Ames, "Safe backstepping with control barrier functions," in *Proc. Conf. Decis. Control*, pp. 5775–5782, 2022.
- [8] M. H. Cohen, R. K. Cosner, and A. D. Ames, "Constructive safety-critical control: Synthesizing control barrier functions for partially feedback linearizable systems," *IEEE Control Systems Letters*, 2024.
- [9] Q. Nguyen and K. Sreenath, "Exponential control barrier functions for enforcing high relative-degree safety-critical constraints," in *Proc. Amer. Control Conf.*, pp. 322–328, 2016.
- [10] W. Xiao and C. Belta, "High order control barrier functions," *IEEE Trans. Autom. Control*, vol. 67, no. 7, pp. 3655–3662, 2022.
- [11] M. H. Cohen, T. G. Molnar, and A. D. Ames, "Safety-critical control for autonomous systems: Control barrier functions via reduced order models," *Annual Reviews in Control*, vol. 57, p. 100947, 2024.
- [12] T. G. Molnar, R. K. Cosner, A. W. Singletary, W. Ubellacker, and A. D. Ames, "Model-free safety-critical control for robotic systems," *IEEE Robot. Aut. Lett.*, vol. 7, no. 2, pp. 944–951, 2022.
- [13] A. Isidori, *Nonlinear Control Systems*. Springer, third ed., 1995.
- [14] A. D. Ames, G. Notomista, Y. Wardi, and M. Egerstedt, "Integral control barrier functions for dynamically defined control laws," *IEEE control systems letters*, vol. 5, no. 3, pp. 887–892, 2020.
- [15] W. Xiao, C. G. Cassandras, C. Belta, and D. Rus, "Control barrier functions for systems with multiple control inputs," in *Proc. Amer. Control Conf.*, pp. 2221–2226, 2022.
- [16] M. Fliess, J. Levine, P. Martin, and P. Rouchon, "A lie-backlund approach to equivalence and flatness of nonlinear systems," *IEEE Transactions on Automatic Control*, vol. 44, no. 5, pp. 922–937, 1999.
- [17] R. M. Murray, M. Rathinam, and W. Sluis, "Differential flatness of mechanical control systems: A catalog of prototype systems," in *ASME international mechanical engineering congress and exposition*, pp. 349–357, Citeseer, 1995.
- [18] T. Lee, M. Leok, and N. H. McClamroch, "Geometric tracking control of a quadrotor UAV on SE(3)," in *49th IEEE Conference on Decision and Control (CDC)*, (Atlanta, GA), pp. 5420–5425, IEEE, Dec. 2010.
- [19] D. Mellinger and V. Kumar, "Minimum snap trajectory generation and control for quadrotors," in *Proc. Int. Conf. Robot. and Autom.*, pp. 2520–2525, 2011.
- [20] G. Wu and K. Sreenath, "Safety-critical control of a 3d quadrotor with range-limited sensing," in *Dynamic Systems and Control Conference*, vol. 50695, p. V001T05A006, 2016.
- [21] G. Wu and K. Sreenath, "Safety-critical control of a planar quadrotor," in *Proc. Amer. Control Conf.*, pp. 2252–2258, 2016.
- [22] A. Alan, A. J. Taylor, C. R. He, G. Orosz, and A. D. Ames, "Safe controller synthesis with tunable input-to-state safe control barrier functions," *IEEE Contr. Syst. Lett.*, vol. 6, pp. 908–913, 2022.
- [23] J. J. Choi, D. Lee, K. Sreenath, C. J. Tomlin, and S. L. Herbert, "Robust control barrier–value functions for safety-critical control," in *Proc. Conf. Decis. Control*, pp. 6814–6821, 2021.
- [24] M. H. Cohen, P. Ong, G. Bahati, and A. D. Ames, "Characterizing smooth safety filters via the implicit function theorem," *IEEE Contr. Syst. Lett.*, vol. 7, pp. 3890–3895, 2023.
- [25] D. Liberzon, *Switching in Systems and Control*. Boston, 2003.
- [26] M. Jankovic, "Robust control barrier functions for constrained stabilization of nonlinear systems," *Automatica*, vol. 96, 2018.
- [27] M. Krstić, I. Kanellakopoulos, and P. Kokotović, *Nonlinear and Adaptive Control Design*. Wiley, 1995.
- [28] R. K. Cosner, I. Sadalski, J. K. Woo, P. Culbertson, and A. D. Ames, "Generative modeling of residuals for real-time risk-sensitive safety with discrete-time control barrier functions," in *Proc. Int. Conf. Robot. and Autom.*, pp. 9960–9967, 2024.
- [29] A. Singletary, A. Swann, Y. Chen, and A. D. Ames, "Onboard safety guarantees for racing drones: High-speed geofencing with control barrier functions," *IEEE Robotics and Automation Letters*, vol. 7, no. 2, pp. 2897–2904, 2022.

APPENDIX

We show that the tracking CLF (40) satisfies (21) for 3D rotation matrices—the result holds for 2D rotation matrices as a special case and as such, holds for all case studies presented in this paper. First, define the *error rotation matrix* \mathbf{R}_e as the rotation matrix which represents the attitude of the *desired* frame with respect to the *body-fixed* frame, i.e.,

$$\mathbf{R}_e = \mathbf{R}^\top \mathbf{R}_{\text{des}}. \quad (48)$$

This rotation matrix can always be represented using Euler angles, that is, it can be represented by a sequence of three (not necessarily unique) rotations about intrinsic orthogonal axes. In particular, we can choose the Z-X-Z rotation sequence, resulting in:

$$\mathbf{R}_e = \mathbf{R}_z(\psi) \mathbf{R}_x(\theta) \mathbf{R}_z(\varphi). \quad (49)$$

Given \mathbf{R}_e , for any Euler angle rotation sequence, the resultant φ and ψ are *not* guaranteed to be unique (specifically when the second Euler angle θ is defined such that it aligns the 1st and 3rd rotation axes). However, θ will always be unique. Next, consider the geometric tracking CLF:

$$V(\mathbf{x}) = \frac{\|\tilde{\mathbf{k}}(\mathbf{x})\|^2}{2} \text{tr}(\mathbf{I} - \mathbf{R}_e), \quad (50)$$

which is a slight modification of the Lyapunov function in [18] used to prove “near” global asymptotic stability of the equilibrium point defined by $\mathbf{R}_e = \mathbf{I}$. Furthermore, for the 3D quadrotor (42), we have $L_{\mathbf{g}_1} L_{\mathbf{f}} \mathbf{y}(\mathbf{x}) = \mathbf{R}_e \mathbf{e}_z$, thus, following from (20), we can express $\|\mathbf{e}(\mathbf{x})\|$ as:

$$\|\mathbf{e}(\mathbf{x})\| = \|(\mathbf{I} - \mathbf{R}_e \mathbf{e}_z \mathbf{e}_z^\top \mathbf{R}^\top) \tilde{\mathbf{k}}(\mathbf{x})\|. \quad (51)$$

Since $\mathbf{b}_z = \mathbf{R}_e \mathbf{e}_z$ is the basis vector representing the body-fixed z-axis, this becomes:

$$\|\mathbf{e}(\mathbf{x})\| = \|(\mathbf{I} - \mathbf{b}_z \mathbf{b}_z^\top) \tilde{\mathbf{k}}(\mathbf{x})\| \quad (52)$$

$$= \|\tilde{\mathbf{k}}(\mathbf{x}) - \mathbf{b}_z (\mathbf{b}_z^\top \tilde{\mathbf{k}}(\mathbf{x}))\|, \quad (53)$$

where the vector $\tilde{\mathbf{k}}(\mathbf{x}) - \mathbf{b}_z (\mathbf{b}_z^\top \tilde{\mathbf{k}}(\mathbf{x}))$ in (53) is the component of $\tilde{\mathbf{k}}(\mathbf{x})$ orthogonal to \mathbf{b}_z . Since the angle between $\tilde{\mathbf{k}}(\mathbf{x})$ and \mathbf{b}_z is precisely the θ in (49), the magnitude of the projection can be expressed as:

$$\|\mathbf{e}(\mathbf{x})\| = \|\tilde{\mathbf{k}}(\mathbf{x}) \sin(\theta)\|. \quad (54)$$

Using this simplified expression for $\|\mathbf{e}(\mathbf{x})\|$, we now present the following Lemma.

Lemma 1. *There exists a $\beta > 0$ such that the tracking CLF (50) is lower bounded by (54) as in (21) for all $\mathbf{x} \in \mathbb{R}^n$.*

Proof. By substituting (49) into (50), and dropping the dependency on \mathbf{x} for brevity, we arrive at:

$$V(\mathbf{x}) = \frac{\|\tilde{\mathbf{k}}\|^2}{2} \text{tr}(\mathbf{I} - \mathbf{R}_z(\psi) \mathbf{R}_x(\theta) \mathbf{R}_z(\varphi)) \quad (55)$$

$$= \frac{\|\tilde{\mathbf{k}}\|^2}{2} (\text{tr}(\mathbf{I}) - \text{tr}(\mathbf{R}_z(\psi) \mathbf{R}_x(\theta) \mathbf{R}_z(\varphi))) \quad (56)$$

$$= \frac{\|\tilde{\mathbf{k}}\|^2}{2} (3 - (\cos(\varphi + \psi) + \cos(\varphi + \psi) \cos(\theta) + \cos(\theta))) \quad (57)$$

$$= \frac{\|\tilde{\mathbf{k}}\|^2}{2} (4 - (\cos(\varphi + \psi)(\cos(\theta) + 1) + (\cos(\theta) + 1))) \quad (58)$$

$$= \|\tilde{\mathbf{k}}\|^2 \left(2 - \left(\frac{\cos(\varphi + \psi) + 1}{2} \right) (\cos(\theta) + 1) \right). \quad (59)$$

Because $\frac{\cos(\cdot)+1}{2}$ exists on the domain $[0,1]$, and $\cos(\cdot)+1$ exists on $[0,2]$, we can say:

$$V(\mathbf{x}) = \|\tilde{\mathbf{k}}\|^2 \left(2 - \left(\frac{\cos(\varphi + \psi) + 1}{2} \right) (\cos(\theta) + 1) \right) \quad (60)$$

$$\geq \|\tilde{\mathbf{k}}\|^2 (2 - (\cos(\theta) + 1)) \quad (61)$$

$$= \|\tilde{\mathbf{k}}\|^2 (1 - \cos(\theta)) \quad (62)$$

$$\geq \|\tilde{\mathbf{k}}\|^2 (1 - \cos(\theta)) \left(\frac{\cos(\theta) + 1}{2} \right) \quad (63)$$

$$= \|\tilde{\mathbf{k}}\|^2 \frac{1 - \cos^2(\theta)}{2} \quad (64)$$

$$= \|\tilde{\mathbf{k}}\|^2 \frac{\sin^2(\theta)}{2} \quad (65)$$

$$= \frac{1}{2} \|\tilde{\mathbf{k}} \sin(\theta)\|^2 \quad (66)$$

$$= \frac{1}{2} \|\mathbf{e}(\mathbf{x})\|^2 \quad (67)$$

$$\geq \beta \|\mathbf{e}(\mathbf{x})\|^2, \quad \forall \beta \in \left(0, \frac{1}{2} \right]. \quad (68)$$

Therefore, the choice of CLF (50) satisfies (21). \square